Enhanced Photocatalytic Degradation of Industrial Dye by g-C_3N_4/TiO_2 Nanocomposite: Role of Shape of TiO_2

A Dissertation submitted
In
partial fulfilment of the requirements for the degree of

Master of Science
in
Chemistry

by

Divya Monga
Registration No.: 301602019

Under the Supervision of

Dr. Soumen Basu

SCHOOL OF CHEMISTRY & BIOCHEMISTRY
THAPAR INSTITUTE OF ENGNEERING AND TECHNOLOGY
PATIALA

June, 2018

CERTIFICATE

I hereby declare that the thesis entitled **"Enhanced photocatalytic degradation of industrial dye by C_3N_4/TiO_2 nanocomposite: Role of shape of TiO_2"** is an authentic record of my work carried out as requirements for the award of the degree of Master of Science in Chemistry at Thapar Institute of Engineering and Technology, Patiala under the supervision of Dr.Soumen Basu, Associate Professor, School of Chemistry & Biochemistry, Thapar Institute of Engineering and Technology, Patiala during July' 2016 to July' 2018. No part of the matter embodied in this report has been submitted to any other university or institute for the award of any degree.

Date: 29 June 2018

Divya Monga

It is certified that the above statement made by the student is correct to the best of my/our knowledge and belief.

Dr.Soumen Basu
Associate Professor,
School of Chemistry & Biochemistry
Thapar Institute of Engineering and Technology, Patiala - 147004

Acknowledgement

First of all, I owe my gratitude to the Head of the Department, **Dr.Amjad Ali** for providing me an opportunity in the form of this dissertation to develop my interest in research.

In the same spirit, I would like to thank my Supervisor, **Dr.SoumenBasu** for his constructive guidance and constant support during the project. The work presented here could not have been accomplished without his patience and ever willingness to teach. He has taught me to be concise and correct in my approach from the formulation of ideas to the presentation of the results.

Special thanks to all the **Teaching Faculty** of the department for their cooperation and guidance.

I would also like to express my gratitude to Ms. Akansha Mehta, Mr. Amit Mishra, Ms. ShagunKainth, Ms. Surbhi and Ms. Aanchal who never turned me down whenever I approached them for any kind of help. Also, thanks to all the research scholars for their assistance.

I am grateful to **Thapar Institute of Engineering and Technology & School of Chemistry and Biochemistry** for providing financial support and all necessary infrastructure and laboratory facilities to carry out the experimental work.

Words fail me to express my thanks to my family and friends who have always supported me and have been a source of strength and inspiration to me during the entire period of the work.

All these thanks are, however, only fraction of what is due to almighty for granting me an opportunity and strength to successfully accomplish this project.

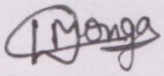

Divya Monga

Abstract

Enhanced photodegradation of RhB dye by using synthesized g-C_3N_4/TiO_2nanocomposite having different shapes of TiO_2, showing role of shape of TiO_2 in photodegradation has been demonstrated in this present work. As TiO_2 has a wide band gap of 3.2 eV and utilize energy of radiations of only UV region of light, so has some limitations as a photocatalyst. To improve the photocatalytic efficiency of TiO_2 we have incorporated g-C_3N_4, a visible light active photocatalyst. The TiO_2 nanoparticles with different shapes (Nanorods, Nanospheres, and Nanotubes) were prepared by different methods. The g-C_3N_4 was prepared by pyrolysis of Urea. The g-C_3N_4/TiO_2 composites were prepared by stirring g-$C_3N_4$and pre-synthesized TiO_2 nanoparticles. The ratio of g-C_3N_4 and TiO_2 nanoparticles is 1:1. On performing photocatalytic experiment we have found that the degradation of RhB dye under visible light irradiation has been increased remarkably upon incorporation of g-C_3N_4 with different shapes of TiO_2. Also, shape of TiO_2 has a remarkable effect in photodegradation. The best degradation performance of ~97% was obtained from g-C_3N_4/TiO_2 (Nanorods) composite. Although, degradation efficiency of composite of other shapes of TiO_2 (Nanospheres and Nanotubes) with g-C_3N_4 were also found to be greater than that of g-C_3N_4/TiO_2 (P25) composite. Results from UV–Vis absorption study, X-ray Diffraction studies, and X-ray photoelectron spectroscopy suggest that the improvement in photocatalytic activity of composite is due to decrease in band gap energy and increased light absorption in visible region. Also there is an increase in electron hole separation efficiency due to effectual interfacial transfer of electron between g-C_3N_4 and TiO_2 (NR, NS, NT) of g-C_3N_4/TiO_2 composites. The BET surface area analyzer, HRTEM, FESEM and Electron Diffraction studies with Color mapping indicate successful incorporation of g-C_3N_4 with TiO_2 in the composites. Results from scavenger study indicate that electron and superoxide ions act as main reactive species in photodegradation of RhB dye by the composite.

Contents

List of Figures

List of Tables

List of Abbreviations and Symbols

1.	**BOD**	Biological Oxygen Demand
2.	**BET**	Brunauer-Emmett-Teller
3.	**RhB**	Rhodamine B
4.	**AOPs**	Advanced Oxidation Processes
5.	**eV**	Electron Volt
6.	**nm**	Nanometer
7.	**^{o}C**	Degree Celsius
8.	**g-C_3N_4**	Graphitic Carbon Nitride
9.	**TTIP**	Titanium tetraisopropoxide
10.	**MB**	Methylene Blue
11.	**LED**	Light Emitting Diode
12.	**EDX/EDS**	Energy dispersive X-ray spectroscopy
13.	**Ɵ**	Theta
14.	**Min**	Minutes
15.	**M**	Molar
16.	**N**	Normal
17.	**h**	Hours
18.	**g**	Gram
19.	**λ**	Wavelength
20.	**λ_{max}**	Maximum wavelength
21.	**K**	Kelvin
22.	**m^2g^{-1}**	Meter square per gram
23.	**µm**	Micrometer
24.	**µL**	Micro litre
25.	**ppm**	Parts per million

26.	**mL**	Millilitre
27.	**MW**	Molecular Weight
28.	**NR**	Nanorods
29.	**NT**	Nanotubes
30.	**NPs**	Nanoparticles
31.	**NS**	Nanospheres
32.	**%**	Percentage
33.	**BJH**	Barrett– Joyner–Halenda
34.	**kV**	KiloVolt
35.	**FESEM**	Field Emission Scanning electron microscope
36.	**mg**	Miligram
37.	**cm**	Centimeter
38.	**STP**	Standard Temperature and Pressure
39.	**HRTEM**	High Resolution Transmission electron microscope
40.	**UV-Vis**	Ultraviolet-Visible
41.	**W**	Watt
42.	**XRD**	X-ray diffractometer
43.	**XPS**	X-ray photoelectron spectroscopy
44.	**a.u.**	Arbitrary Units

CHAPTER 1

Introduction

Now a day, saving water is most important to save our planet and future of mankind. The world is achieving new heights with the development of science, technology, society and mankind but at the cost of our important resources. Environmental disorders are one of the results of this rapid growth is out of which pollution of air, water etc. is a big problem. Human activities have caused a great harm to our natural resources e.g. water. There seems to be a crisis of the freshwater resources due to their fast depletion. Water pollution is a worldwide problem therefore removal of pollutants from water is the necessitous and for this developing a cost effective and environmentally safe method is a challenging task [1].

People working for water purification and environment are concerned for our water resources constituting both groundwater and polluted wastewaters. For this, now water quality norms now become very strict against the hazardous pollutants in many countries. Now a day, with increasing revolution in science and technology there is a high demand in industries for newer chemicals to be used to control water pollution [2].

1.1 Dyes

Use of synthetic dyes is prominent in almost all fields of the consumer goods sector [3]. Worldwide there is production of about 45000 tons of organic dye yearly, greater than 11% of its is lost as effluvium in water bodies [4].There are wide range of activities in a textile industry from preparation of textile material to its dyeing and finishing. All these activities are highly polluting and also consume large amount of energy and water [5].The effluents from these processes are usually harmful, highly colored, mutagenic or carcinogenic. Substantial environmental hazards are caused by these waste waters because of their strong colors greater chemical oxygen demand (80% is because of supplementary dyeing agents like starch and $C_2H_3NaO_2$ and 20% is due to dyes) and complex chemical nature of effluents [6].The dyes affect photosynthesis by changing the absorption and reflection of sunlight on the water. Also there are

other quality indicators such as biological oxygen demand (BOD) that are also important to evaluate the water quality.

On basis of the chromophores present in them, these dyes were divided in 20-30 groups. Some important are phthalocyanine, anthraquinone, triarylmethane dyes and azo (mono, di, tri and ploy) azo dyes [3] (Figure 1).

Textile dyestuffs can be grouped into 10 categories or classes: Basic Dyes, Acid Dyes, Direct Dyes, Vat Dyes, Mordant Dyes, Reactive Dyes, Azoic Dyes, Disperse Dyes, Sulphur Dyes, and Pigment Dyes [7].

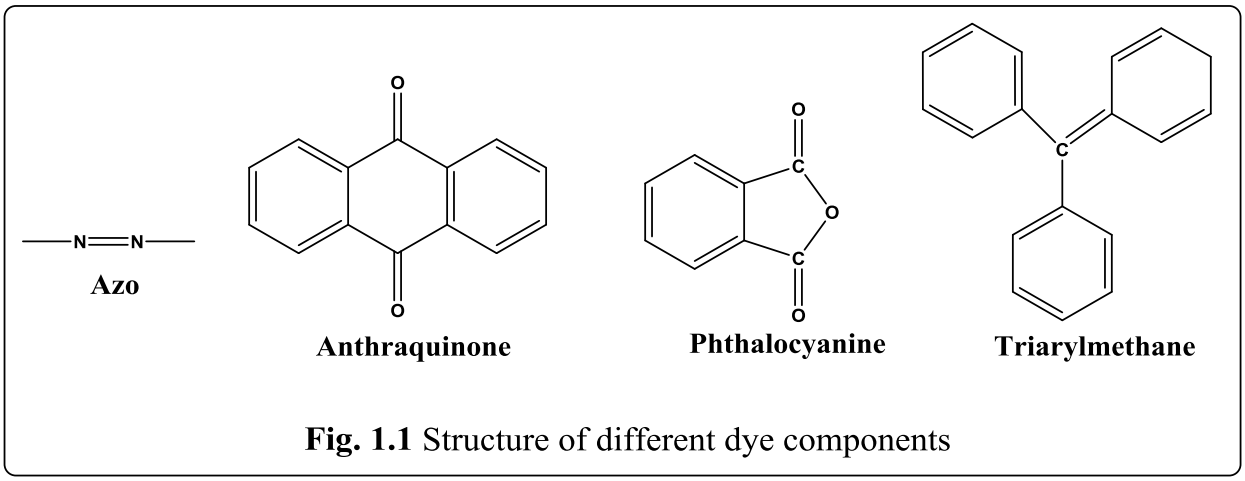

Fig. 1.1 Structure of different dye components

1.1.1 Rhodamine B Dye

Rhodamine B (RhB), one of the most commonly used dyes is extensively used for industrial purposes, such as paint, paper, printing and dyeing, leathers etc. Rhodamine B is an example of basic dye [8]. RhB is a good water tracer fluorescent and is extensively used as a colorant in food, paper and textiles industry [9]. It is harmful for animals and human beings, and causes skin irritation, respiratory tract and eye infections. It also causes the carcinogenicity, neurotoxicity and developmental disorders in living beings [10]. The λ_{max} of RhB Dye comes near 555nm.

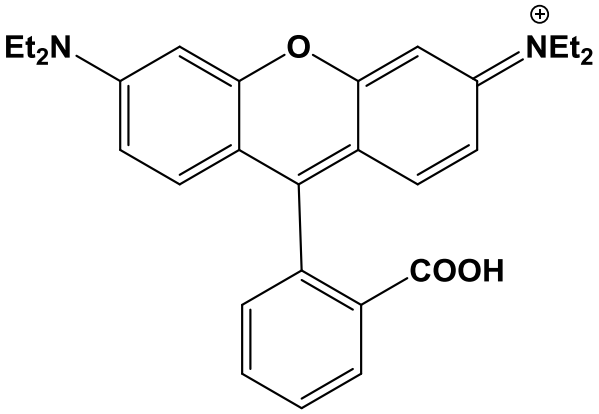

Fig.1.2 Structure of Rhodamine B Dye

One of the major problems with the dyes is that they are exceptionally stable in sun light and also during washing. Also they oppose the effect of microbial attack. So that, they aren't degraded easily and they are not readily removed from wastewater by frequently used effluent treatment systems [11].

1.2 Conventional Effluent Treatment Method

1.2.1 Physical Methods: Physical methods of separation are use to separate some heavy materials and others easily separable materials from the wastewater. These methods involve [5]:

i. **Filtration**
ii. **Coagulation-Flocculation**
iii. **Adsorption**
iv. **Ion Exchange**

1.2.2 Chemical Methods: Chemical methods involve degradation and removal of various dyes, metal ions etc. from wastewater [5].

i. **Ozonation**
ii. **Chemical oxidation**
iii. **Advanced Oxidation Processes (Photochemical and Photocatalytic)**

iv. **Fenton's Reaction**

v. **Electrochemical oxidation**

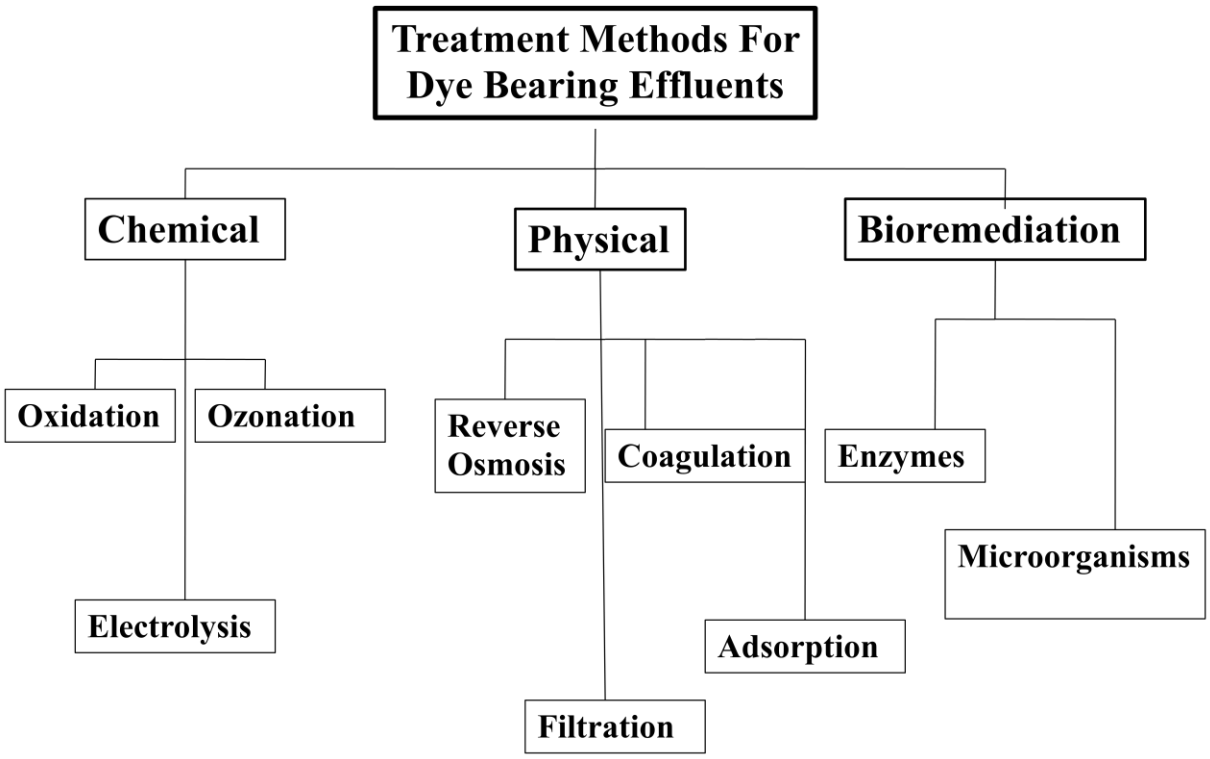

Fig.1.3 An overview of methods for treatment of dye bearing effluents

1.2.3 Bioremediation: Use of microbes for degradation of organic pollutants is called bioremediation.

For degradation of organic pollutants from water, AOP's [12] have been appearing to be most effective for near complete degradation [13, 14]. In Advanced Oxidation Process, the technique which has great capability for degradation of organic pollutants is semiconductor photocatalysis. There are many advantages of AOP's over other conventional oxidation processes, like (1) degradation process requires only solar or near UV-light, (2) no requirement of addition of any other chemicals, (3) complete mineralization of the pollutants, and (4) works at room temperature [15, 16].

1.3 TiO_2 Nanoparticles as Photocatalyst

Semiconductors such as TiO_2 or ZnO are commonly used as catalytic agents because of their low costs, high stability, high efficiency and very less toxicity [17]. TiO_2 is a powerful photocatalyst because of its high oxidizing power, long-term photostability, and non-toxicity. The organic pollutants can be degraded into less toxic and easily biodegradable compounds of low molecular weight by using TiO_2 catalyst [18, 19]. The physical, structural and chemical properties of TiO_2 nanoparticles determine some of its specific applications. Rutile, anatase and brookite are the three crystalline phases of TiO_2. The thermodynamic stable state is rutile, while the anatase and brookite are metastable states. The phase crystallite size, structure, pore structure, and specific surface area of TiO_2 determine its photocatalytic activity. [5].

One further important advantage of TiO_2 is the fact that the process of photocatalysis can be powered by natural sunlight also, thus significantly reducing the electrical power requirements and lowering the operating costs [20]. Nano-TiO_2 can photocatalytically oxidize organic compounds, when used with light. Different types of nanomaterials can be prepared from TiO_2, including nanoparticles, nanotubes, nanorods, nanowires, nanospheres and mesoporous and nanoporous TiO_2 containing materials [21].

1.4 Limitation of TiO_2 as Photocatalyst

To some extent, the worldwide technological use of TiO_2 is compelled by its wide band gap of ~3.2 eV, and for photocatalytic activation, it shows low efficiency in utilizing sunlight as it require irradiation of UV light [20]. Due to the following limitations of TiO_2: 1) less adsorption ability of hydrophobic pollutants; 2) difficulty of separation and recovery; and 3) high aggregation tendency, some of the practical applications were also hindered [22]. Only radiations having wavelength of less than 390 nm can be utilized by TiO_2, this makes only 5% of solar light. This is because of its wide band gap [23].

1.5 Incorporation of g-C_3N_4

To increase the photocatalytic efficiency of TiO_2, we need a photocatalyst which is powerful and visible light-active like graphitic carbon nitride (g-C_3N_4), a polymeric semiconductor. Due to its potential application in photochemistry, g-C_3N_4 has attracted concentration of researchers [24,

25]. This organic semiconductor can be used as a promising photocatalyst activated under visible light irradiation. Because of its simple and easy synthesis, high physicochemical stability, fascinating electronic band structure and "earth-abundant" nature, it is extensively used as a photocatalytic material. The energy band-gap of carbon nitride was estimated to ~ 2.7 eV by Wang et al, which is very less than band gap of TiO_2 particles [26, 27]. Urea was found as the economical source for production of carbon nitride (C_3N_4) nanosheets. Urea can be converted into carbon nitride by pyrolysis [28].Therefore, to attain the enhanced light harvesting capacity and enhanced charge separation of TiO_2, it is suitable to couple g-C_3N_4 with TiO_2semiconductor [29].Many ideas were proposed to unite the great photocatalytic activity ofTiO_2 nanoparticles and the high surface area with good electron/hole transfer capability of g-C_3N_4, to form g-C_3N_4/TiO_2 nanocomposite (a new efficient photocatalyst) [30, 31].

1.6 Thesis Objectives

For comparative study we have prepared a series of catalysts having g-C_3N_4 combined with different shapes of TiO_2 (like nanorods, nanospheres, and nanotubes and DeggusaP25) and its activities are compared with the photocatalytic activity of C_3N_4 and P25 alone.

The composite's structure and composition was characterized and evaluated using X-ray Diffraction (XRD), Brunauer–Emmett–Teller (BET) isotherms, Energy Dispersive X-ray spectroscopy (EDS). Oxidation state of elements was determined by X-ray photoelectron spectroscopy (XPS). The surface morphology was studied by using High Resolution Transmission Electron Microscopy (HRTEM) and Field Emission Scanning Electron Microscopy (FESEM). Photocatalytic efficiency of the prepared photocatalysts was determined by studying the degradation of Rhodamine B dye under visible light irradiation.

Mechanism of the degradation is determined by Scavenger study. Also, the effect on the photocatalytic activity by different catalyst concentration and pH of dye solution and reusability of catalyst was investigated.

CHAPTER 2

Literature Review

An immediate problem facing humanity is the lack of clean and accessible water. Water covers about 70% of earth's surface, however out of this only 1% is suitable for human consumption [Shiklomanov et al., 2000]. The world's water supply is under considerable stress due to increasing industrialization, increasing demand, and a decreasing supply due to pollution. This can be a threat to our health and environment. It has become the matter of our social and economic concern [Chen, D. & Ray, A. K., 1999].

Textile industry is one of the rapidly developing industrial sectors. It is a remarkable contributor to many national economies; encircle both small and large-scale operations worldwide. Dyestuffs and other trading colorants have come out as an interest of environmental remediation attempts [Nasr et al., 1996].

Textile industries release these untreated effluents which are highly coloured and contain significant amount of contaminants in it that pollute water bodies. These effluents are visible in water even when present at very low concentration and also degradation products of these dyes are often carcinogenic (Kim et al. 2003). To remove these pollutants from wastewater many methods have been described some of them are adsorption, membrane filtration, precipitation, coagulation/flocculation, ultrasonic, ion exchange, flotation, electrolysis, mineralization, advanced oxidation processes and chemical reduction. However, these approaches often involve complicated procedures (Cheima Fersi and Mahmoud Dhahbi 2008).

The technologies which are presently used to degrade the dye in contaminated water includes the following processes 1.primary (adsorption, flocculation), 2.secondary (biological methods), and 3.chemical processes (like chlorination, ozonization) [More et al., 1989; Patil and Shinde et al., 1988]. However these methods are non-destructive, because they give rise to new type of pollution by only transferring the non-biodegradable matter into slime, which require further treatment [Chaudhuri and Sur, 2000; Arslan et al., 2000; Stock et al., 2000].

So some other techniques like Advanced Oxidation Process(AOP) has gain attention from various different sectors of scientific community as it produces remarkably less residuals as compared to the classical methods and is easy to handle. Amongst the several techniques utilized in the AOP approach are the radiation induced degradation of dyes [Vahdat et al., 2010; Mohamed et al., 2009; Chen et al., 2008; Dajka et al., 2003], UV photolytic technique [Elmorsi et al., 2010; AlHamedi et al., 2009 ; Gul and YildIrIm, 2009] and photocatalytic approach [Raufet al., 2010; Xu et al., 2010; Zhang et al., 2009; Bukallah et al., 2007; Habibi and Talebian, 2007] which are under main consideration.

2.1 Treatment of Organic Dyes

An excellent method for treatment of environmentally toxic materials is the Advanced Oxidation Process (Daghrir et al., 2013). Observing dye instability for the first instance by the photocatalytic reduction of Methylene Blue dye to the leuco form in the presence of an illuminated inorganic semiconductor TiO_2 and CdSb was reported by Pamfilov et al., (1969) and Yoneyama et al., (1972) respectively.

Many attempts have been investigated to degrade the organic dye photochemically from wastewater. The photoreduction of Methyl Orange to a hydrazine derivative in presence of colloidal TiO_2 and photoinduced transfer of electron from TiO2 to Methyl Orange (λ_{max} = 470 nm) results in the bleaching of the dye, this was reported by Brown and Darwent, (1984a & b). However in the late 1990s the field legitimately “took off”. As documented by more than 2000 publications [Blake, 2001], fundamental and applied research on this area in all over the world has been performed extensively during the last twenty years.

The photocatalytic degradation process has appeared as a versatile and potentially influential technique for dealing with the problem of different types of dye containing wastewater. A number of research groups have dealt with the photocatalytic reduction of these dyes in the presence of UV or visible light with very good results [Davis et al., 1994; Vinodgopal et al., 1996; Zhang et al., 1998].

2.2Semiconductor Photocatalysts

Akihiko Kudo and Yugo Miseki synthesize heterogeneous photocatalyst materials with different metal ions like Ti^{4+}, Zr^{4+}, W^{6+} for water splitting in 2008. Direct splitting of water by an oxide semiconductor ($In_{1-x}Ni_xTaO_4$) photocatalyst under irradiation of visible light is shown by Zhigang Zou et al. 2001. In 2008, Peng Wang et al. showed that in visible light, Ag@AgCl can act as a highly active and stable catalyst for photodegradation. Solid Solution of GaN:ZnO is a good photocatalyst for Water Splitting under visible light [Kazuhiko Maeda et al. 2005].

In many photocatalytic studies commercially accessible samples of TiO_2 (Degussa P-25) have been widely used [Rajeshwar et al., 2008]. The photoreactivity of Degussa P25 TiO_2 works the best in environmental applications (Martin 29 et al., 1994a & b).Because of its (i) reasonably well defined nature (i.e. BET surface area of 55 for anatase : rutile 70:30% mixture} 15 m^2g^{-l} typically nonporous and 30 nm crystallite sizes (0.1 μm diameter) aggregates and (ii) a significantly greater photocatalytic activity as compared to other easily available samples of TiO_2 [V.Brezováet al., 1997].

The decolourization of some reactive textile dyes namely Procion Brilliant Magenta M-B (PBM), Procion Brilliant Orange M-2R (PBO), and Procion Brilliant yellow M-4G (PBY) reported by Sivakumar and Shanthi, (2001) using different grades of TiO_2 semiconductor (CDH, DEGUSSA and CERAC) as catalyst under sunlight and concluded that TiO_2 (Degussa P-25) was better than any other grade.

It was explained on the basis of the slow electron-hole recombination in case of Degussa P25. Zielinska et al., (2003, 2001) reported less activity of Tytanpol A11 than Degussa P25 for the photocatalytic decomposition of various organic dyes (Acid Black, Direct Green 99, Reactive Red 198, Acid Blue 7 and Reactive Black 5). This is due to different physical properties of the two titania materials. Bouanimba et al., (2011) compared the efficiency of P25-Degussa and PC500-Millennium photocatalysts and reported the higher efficiency of TiO_2 P25 than TiO_2 from Millennium for the degradation of Bromophenol blue.

Nano-TiO_2 modified with folic acid has the ability kill cells when photoinduced is revealed by Lai and Lee in 2009. Li et al. in 2012 synthesized TiO_2 codoped with nonmetal (like carbon) and metal ions (like molybdenum) by hydrothermal treatment processes. Heat treated TiO_2can act as

a photocatalyst and its photocatalytic activity was investigated by Devi and Krishnaiah in1999 by the photodegradation of two azo dyes (p-Hydroxy-azo-benzene and p-Aminoazo-benzene).

Decomposition of aspirin by immobilized polymeric TiO_2 is prepared and characterized by Mukherjee et al. in 2013 under UV and visible light. (Neppolian et al., 2002) investigated the photocatalytic degradation of three trading textile dyes with different structures using TiO_2 (Degussa P25) photocatalyst in aqueous solution under solar irradiation as a function of COD reduction.

Heterogeneous photocatalysis uses semiconductors as a photocatalyst. There are different photocatalysts utilized in this process, among them TiO_2 has been shown to have the highest effectiveness in removing harmful compounds (Mehrotra and Ray et al., 2003).

2.3 Different shapes of TiO_2 semiconductor

As different shapes of TiO_2 have different properties, so different shapes of TiO_2 have been prepared and their activities were observed. TiO_2 nanotubes were synthesized and characterized by Shahrara Afshar and Moones Hakamizadeh in 2008, they have prepared TiO_2 nanotubes from different precursors namely nanopowder anatase TiO_2, TiO_2 (Degussa P25) and industrial anatase TiO_2 (COSMO) by two treatments: hydrothermal and chemical.

Poulomi Roy et al. 2011 synthesized TiO_2 nanotubes by simple electrochemical oxidation of metallic titanium reactants and its properties and applications were also studied. In 2005, Sangjin Han et al. synthesize highly crystalline TiO_2 nanocrystals at low-temperature and study their application for photodegradation. They have prepared different types of TiO_2 nanocrystals from the same precursor titanium tetraisopropoxide (TTIP) by using different additives and applying different conditions.

JJ Chao et al. 2011 report hydrothermal synthesis of TiO_2 nanorod arrays by titanium butoxide as titanium source on transparent conducting substrates. Zewei Yang et al. 2015 showed Crystal-Controlled synthesis of TiO_2 Nanorods via hydrothermal method. They also show that rutile and brookite are highly efficient photocatalysts. Similarly, Jiarui Huang et al. 2015 report simple synthesis of porous TiO_2 nanospheres and also studied their photocatalytic activity.

In 2017, Xiaojia Li, Mingming Zou and Yang Wang report Synthesis of Mesoporous Anatase TiO_2 Nanospheres by Soft-Template method and showed its enhanced photoactivity. N. Santhosh et al. 2017 synthesize microwave-assisted hydrothermally prepared mesoporous TiO_2 nanospheres. They also have many applications in dye sensitized solar cells.

2.4 Graphitic Carbon Nitride (g-C_3N_4)

Due to application of Graphitic carbon nitride in photochemistry, it has attracted a lot of attention in recent years. S. C. Yanet al. 2009 prepared fabricated g-C_3N_4 by directly heating Melamine and its photodegradation performance was also determined. Activity of g-C_3N_4 as photocatalyst has become recognizable in recent years. S. C. Yanet al.2010 prepared Boron-Doped g-C_3N_4 and use it for photodegradation of RhB and methyl orange dyes under irradiation of visible light.Shaowen Cao and Jiaguo Yu* in 2014 showed Hydrogen Generation from g-C_3N_4 based photocatalyst.

2.5 Composite of g-C_3N_4 with TiO_2

Composite of g-C_3N_4/TiO_2 were prepared by Xifeng Lu, Qilong Wang, and Deliang Cui in 2010. They hydrolyze g-C_3N_4 precursors and $Ti(OC_4H^n{}_9)_4$ in nitrogen atmosphere at room temperature. HongjianYan and HaoxinYang in 2010reported evolution of H_2 by photocatalysis with prepared TiO_2/g-C_3N_4 nanocomposites under visible light irradiation.

g-C_3N_4 and TiO_2 hybrid structures synthesized by simple impregnation method when used for the degradation of phenol under UV irradiation showed good photocatalytic activities [C. Miranda et al., 2013]. Na Yang et al.2011, synthesize N-doped TiO_2/C_3N_4 composite. They first hydrolyze $TiCl_4$ and C_3N_4 at different weight ratios and then heated the hydrolysis product to get the composite. The composite showed enhanced photocatalytic properties. KaiDai et al. 2014 reported degradation of organic pollutants by facet coupled g-C_3N_4/surface-fluorinated TiO_2 nanosheets heterojunction under visible LED light irradiation.

CHAPTER 3

Materials and Methodology

3.1 Materialsand Reagents:

Reactive Rhodamine B dye ($C_{28}H_{31}ClN_2O_3$, λmax = 555nm) was purchased from LOBA CHEMIE PVT. LTD. and is used without any further treatment. Degussa P25 was purchased from Evonik Industries (Hanau, Germany). All other chemicals that were used in experiment are of analytical grade. Urea (Ultrapure CH_4N_2O) was purchased from Spectrochem Pvt. Ltd. Mumbai. Titanium tetraisopropoxide (TTIP) was purchased from Sigma Aldrich (USA), Pluronic P_{123} polymer (PEG-PPG-PEG) was Sigma Aldrich (USA), Titanium (IV) butoxide was purchased from Sigma Aldrich (USA).

3.2Methodology:

3.2.1Preparation of g-C_3N_4: Firstly, 12g of urea dissolved in 50 ml of water was taken in a crucible and placed in a hot air oven for 12 hours for recrystallization. After recrystallization, place this urea in an aluminum crucible and covered with aluminum foil to prevent sublimation of urea, and then heat it at 550 ^{0}C for 2hours at 10 ^{0}C/ min rise in temperature in a muffle furnace [32]. Using a mortar-pestle, the resulting g-C_3N_4 (orange-yellow colored) was grounded into a fine powder. This g-C_3N_4can be used for experimental purpose without any further treatment.

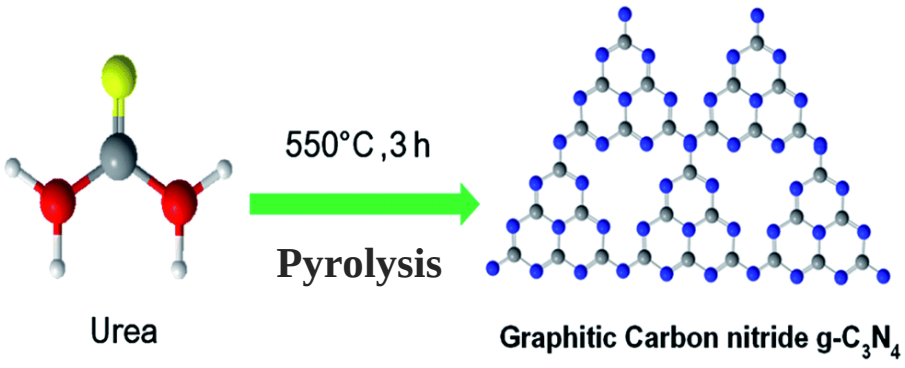

Fig.3.1 Synthesis of graphitic carbon nitride from urea by pyrolysis

Preparation of different shapes of TiO_2 (nanorods, nanotubes, nanospheres):

3.2.2 <u>Preparation of TiO_2 Nanorods</u>: 20ml of titanium tetraisopropoxide (TTIP) was added in 100ml of an aqueous solution of 1M acetic acid containing 4g of pluronic P_{123} ($PEO_{20}PPO_{70}PEO_{20}$) at room temperature. P_{123} controls the hydrolysis and condensation of TTIP precursor. The resulting reaction mixture was stirred for 24 hours and the product was retrieved by filtration. To remove the excess P_{123} polymer the powdery product was washed with excess of ethanol and dried at 85^0C for 2 hours to get final TiO_2 nanorods [33].

3.2.3 <u>Preparation of TiO_2 Nanotubes</u>: 0.5 g of Degussa P25 were treated with 50 ml of 10N NaOH solution and refluxed in an oil bath at 130^0C for 20 and 72h with stirring. After treatment and cooling, the product was washed with ethanol, deionised water, 0.1or 1N HCl and then again with deionised water respectively. The product is then dried in a hot air oven for 2-3h at 80^0C. The dried product is then crushed with a mortar pestle to get powdered TiO_2 nanotubes [34].

3.2.4 <u>Preparation of TiO_2 Nanospheres</u>: They are prepared by template synthesis approach. Firstly 1ml of titanium butoxide is mixed in 22.2 ml of ethylene glycol and stirred vigorously for 8 hours at room temperature. This mixture was poured quickly in a conical flask containing 100ml acetone, 1.5ml distilled water and 0.4ml acetic acid. Stir the mixture at room temperature for 3 hours to form titanium glycolate spheres. Now, these spheres were stirred for 8 hours at 70^0C to produce TiO_2 nanospheres and they were washed many times with distilled water and then dry it in a hot air oven at 100^0C [35].

3.2.5 <u>Preparation of nanocomposite of g-C_3N_4 with TiO_2 (nanorods, nanotubes, nanospheres and P25):</u>

0.1g of TiO_2 (nanorods, nanotubes, nanospheres or P25) was added in 10ml of ethanol and stirred for 1hour. After stirring, 0.1g of g-C_3N_4 (ratio of g-C_3N_4/TiO_2 is 1) was incorporated into the solution and firstly sonicate this mixture for about 30 minutes and then stir the reaction mixture for 3 hours at room temperature. Wash the products with distilled water after stirring and then dried at 60^0C in a hot air oven for 5-6 hours. All the composites were prepared in same manner [6].

3.3 Catalyst characterization

X-Ray Diffraction analysis (XRD) of g-C_3N_4/TiO_2 (NR) catalyst was performed using. X-ray diffractometer having Ni filtered Cu Kα radiations (λ = 0.1504 nm) at 30^{o}C. BET surface area analyzer of Autosorb-1, Quantachrome Instruments, USA was used to analyze surface area of the compounds, at −196 °C. To get a clean surface for adsorption isotherm the samples were first pretreated at 523 K. Barrett– Joyner–Halenda (BJH) model was observed to calculate the pore size distribution from N_2 desorption isotherms. High Resolution Transmission Electron Microscopy (HRTEM) and Field Emission Scanning Electron Microscope (FESEM) has been carried out for the detailed structural analysis of g-C_3N_4/TiO_2 (NR) catalyst through using a ZEISS, by the accelerating at a voltage of 5kV. To analyze the oxidation state and chemical composition of g-C_3N_4/TiO_2 (NR) catalyst XPS was used. XPS spectrometer (KRATOS Axis 165 Shimadzu, UK) was used to obtain the XPS spectra of the g-C_3N_4/TiO_2 (NR) photocatalyst through Mg Kα radiations of 1252.6 eV at 75 W.

3.4 Photocatalytic study

Add 2 mg of catalyst (desired amount) in aqueous solution of Rhodamine B Dye (5ml of 5ppm) and stir the solution in complete dark for 20 minutes to establish adsorption-desorption equilibrium. Irradiate the reaction solution of all the prepared catalyst with visible light at different time intervals upto 80 minutes. Now, filter the catalyst using 0.45- μm nylon filters. UV-Vis spectrophotometer (Specord- 205 Analytik Jena) was used to observe the change in dye concentration (absorbance) [36]. To calculate the photodegradation efficiency following formula is used:

$$R = \{(C_0 - C) / C_0\} \times 100 = \{(A_0 - A)/ A_0\} \times 100$$

Where C_0 and C are the concentration and

A_0 and Aare the absorbance of Rhodamine B dye at 0 and t reaction time, respectively.

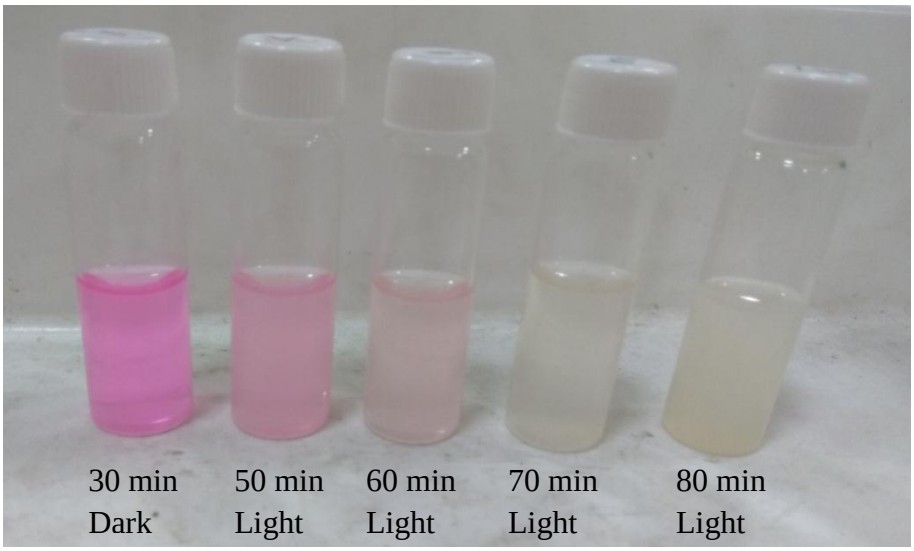

Fig. 3.2 Showing Rhodamine B Dye after 30 minutes of dark adsorption, followed by 50, 60, 70, and 80 minutes of photodegradation respectively.

CHAPTER 4

Results and discussion

4.1Characterization of catalysts

4.1.1 Nitrogen adsorption/desorption analysis

The Brunauer–Emmett–Teller (BET) isotherm of the different shapes TiO_2 and TiO_2/g-C_3N_4 catalysts is shown in Fig.4.1.1a. and 4.1.1b. The isotherms of all other samples shows that they possess Langmuir type IV isotherm indicating mesoporous nature of nanocomposites whereas g-C_3N_4/TiO_2(nanorods) nanocomposite isotherm shows that it possess Langmuir type II isotherm indicating microporus nature of the composite.

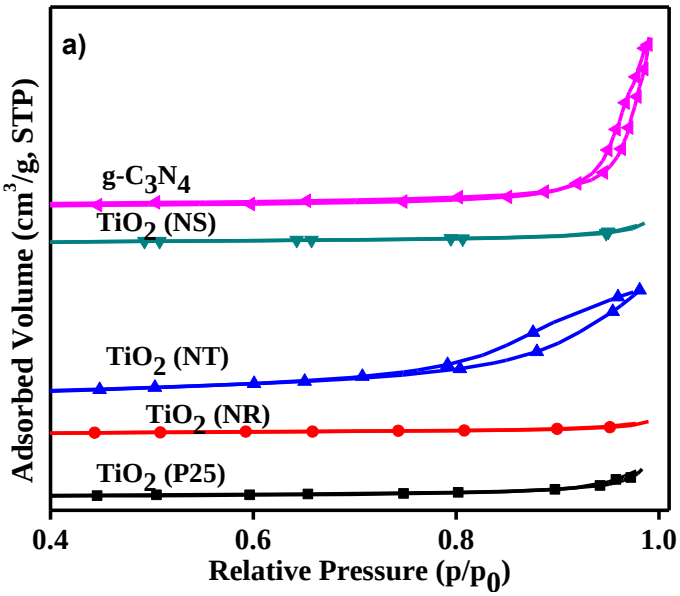

Fig. 4.1.1a BET adsorption isotherm of TiO_2 (P25), g-C_3N_4 and Different Shapes of TiO_2 (NR, NT, and NS)

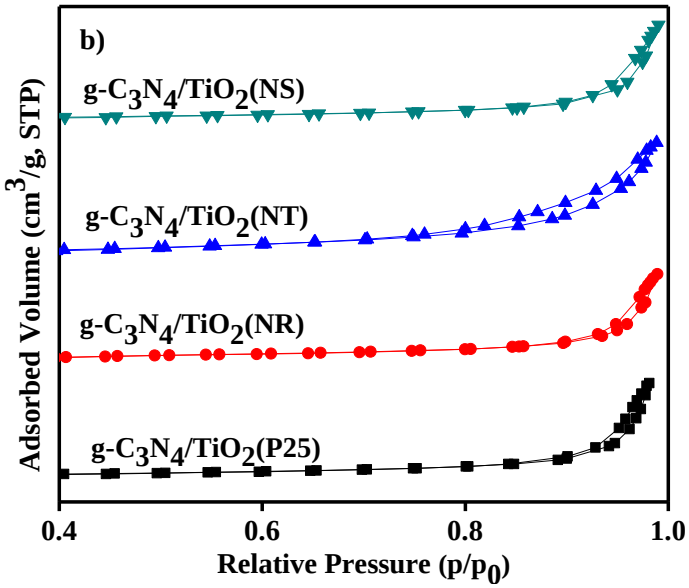

Fig.4.1.1b BET adsorption isotherm of composite of g-C_3N_4 with TiO_2 (P25) and different shapes of TiO_2 (NR, NT and NS).

The values of pore volume, specific surface area and mean pore diameter of as-prepared g-C_3N_4/TiO_2 (nanorods, nanotubes and nanospheres) catalysts are given in Table 4.1.1. It is observed from the data that pore volume and surface area of g-C_3N_4/TiO_2 catalysts tend to increase upon incorporation of g-C_3N_4 on TiO_2 as compared to pore volume and surface area of TiO_2 alone.

Table 4.1.1 Specific surface area, mean pore diameter, and pore volume of g-C_3N_4, TiO_2 (P25) and composites of g-C_3N_4/TiO_2 (P25, NR, NT and NS)

	g-C_3N_4	TiO_2 (P25)	g-C_3N_4/TiO_2 (P25)	g-C_3N_4/TiO_2 (NR)	g-C_3N_4/TiO_2 (NT)	g-C_3N_4/TiO_2 (NS)
Specific surface area (m^2/g)	68.941	30.73	69.001	126.1	137.18	81.196
Mean Pore Diameter (nm)	40.555	13.757	25.598	10.358	14.896	9.3487
Pore Volume (cm^3/g)	0.8217	0.1481	0.4046	0.4311	0.5125	0.4687

BJH plots illustrate the pore size distribution of g-C_3N_4/TiO_2 (nanorods, nanotubes, nanospheres) nanocomposites Fig.4.1.1(c and d).

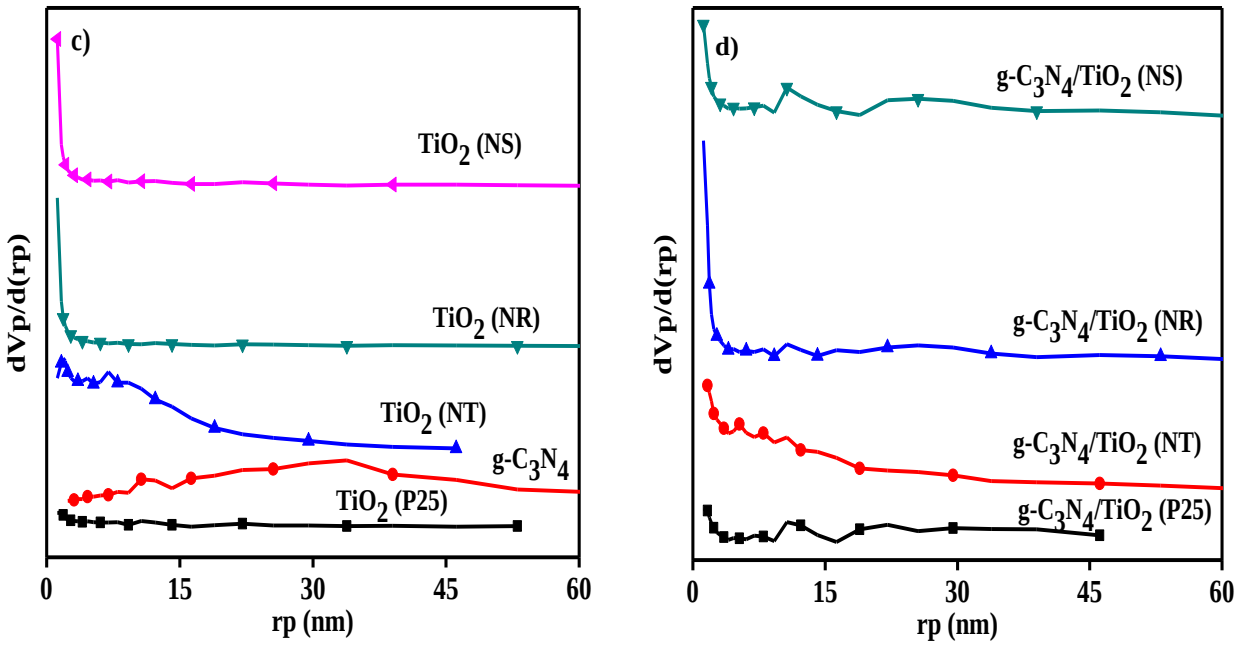

Fig. 4.1.1(c and d) BJH pore size distribution curve for g-C_3N_4, TiO_2 (P25, NR, NS and NT) and composite of g-C_3N_4 with TiO_2 (P25, NR, NS and NT)

4.1.2 XPS of g-C_3N_4/TiO_2 (NR) nanocomposite:

The XPS spectra of the g-C_3N_4/TiO_2 (NR) nanocomposite are shown in Fig. 7. In Fig.4.1.2e the XPS spectrum of g-C_3N_4/TiO_2 (NR), shows that the sample primarily consists of Ti, O, C, and N elements. The spectrum of C1s in Fig. 4.1.2b shows two peaks, one at 284.23 eV corresponds to the adventitious carbon whereas other peak at 287.8 eV corresponds to N-C=N coordination in g-C_3N_4. Spectra of N1s in Fig.4.1.2c also shows two peaks, one at 398.17 eV belongs to C=N-C bonding while other at 399.71 eV corresponds to N-$(C)_3$. The high resolution spectrum of O1s in Fig.4.1.2a shows two peaks, one main peak of high intensity attributing to the Ti-O bond at around 531.3 eV, and a small peak of lesser intensity which is due to O-H bond of water molecules(or due to Ti-O-H bond) around 533 eV. Fig.4.1.2d shows the Ti2p spectrum with two peaks, one at a binding energy of 458.33 eV which belongs to the Ti $2p_{3/2}$ and other at 464.13 eV, which belongs to Ti $2p_{1/2}$.

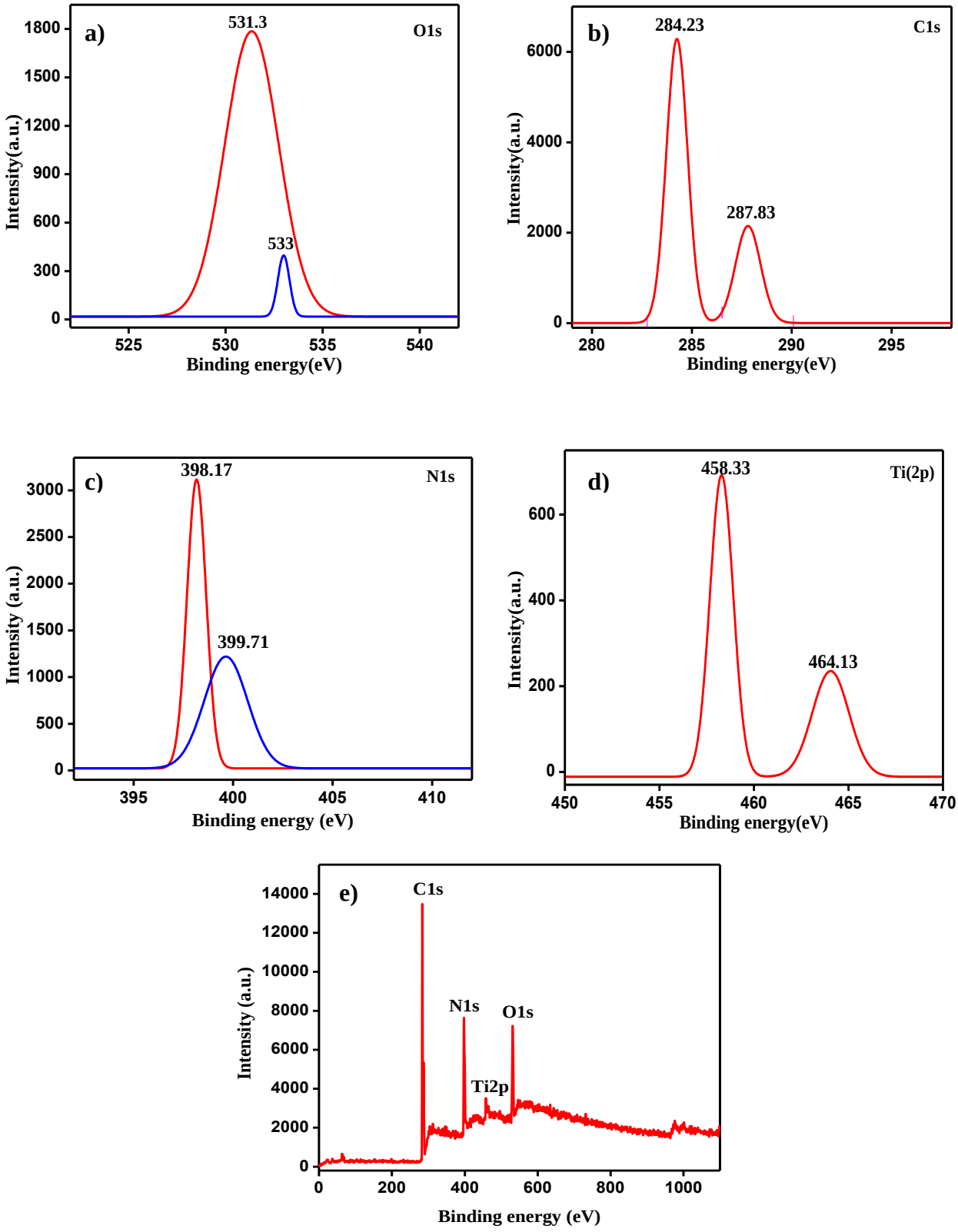

Fig. 4.1.2(a-e) High Resolution XPS Spectrum of g-C_3N_4/TiO_2 (NR) catalyst a) O1s, b) C1s, c) N1s, d) Ti2p and e)survey spectra of g-C_3N_4/TiO_2 (NR) nanocomposite

4.1.3FESEM, HRTEM and ED analysis:

FESEM and HRTEM micrographs of g-C_3N_4/ TiO_2 (nanorods) nanocomposite are exhibited in Fig. 4.1.3(a-d), respectively. It can be seen that smaller nanoparticles of g-C_3N_4 assemble these TiO_2 nanorods (Figure 4.1.3b). Fig.4.1.3a. Indicate that there is a lamellar texture of g-$C_3N_4$with smooth surface. There was strong anchoring of TiO_2 nanoparticles onto the g-C_3N_4 that during the sample preparation for TEM analysis, ultrasonication can't remove these nanoparticles from the g-C_3N_4 surface, indicating the efficient incorporation of g-C_3N_4 on TiO_2 nanorods. Fig.4.1.3b shows presence of thread like nanorods. Fig.4.1.3c shows TEM image of TiO_2 nanorod having width of 17.35 nm. The ED results in Fig.4.1.3dconfirm the successful incorporation of g-C_3N_4 on TiO_2 as well as the purity of the nanocomposites.

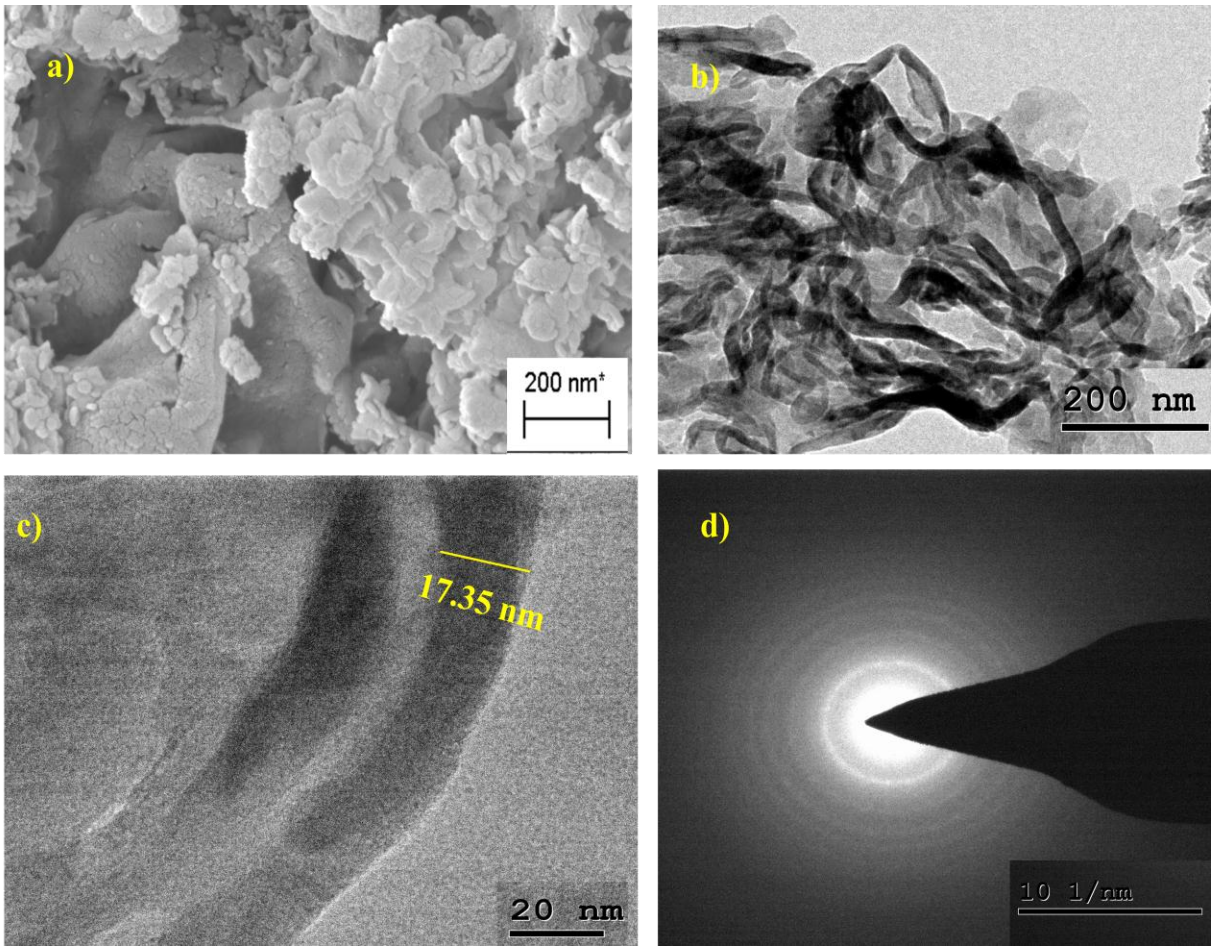

Fig. 4.1.3(a-d) FESEM, HRTEM and ED micrographs a) FESEM image, b) and c) HRTEM images of g-C_3N_4/TiO_2(Nanorods) at 200nm and 20nm respectively, and d) ED image of g-C_3N_4/TiO_2(Nanorods) Composite.

4.1.4 Electron Diffraction Spectroscopy and Elemental mapping spectra.

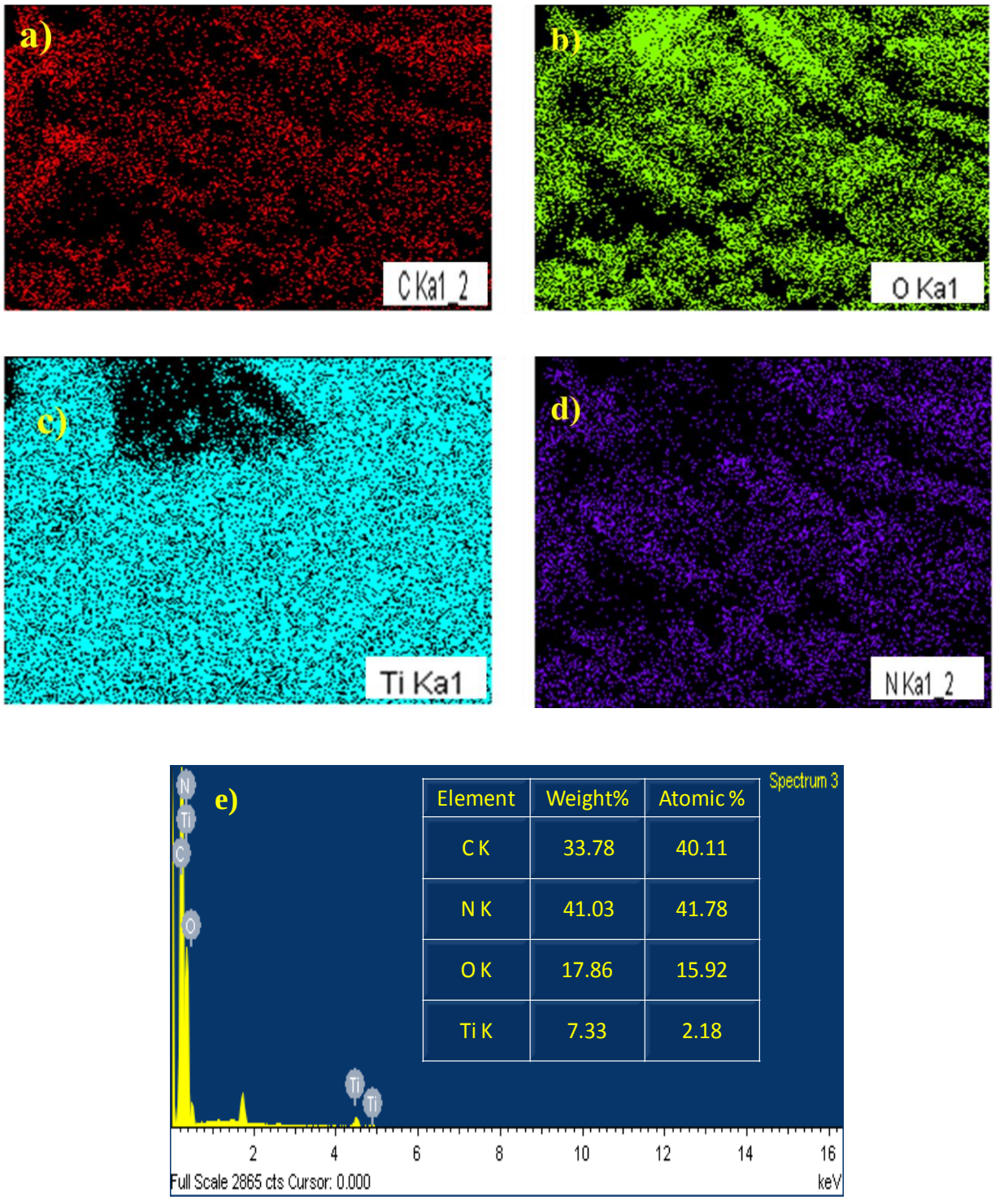

Fig.4.1.4 (a-e) EDS and Elemental mapping spectra of g-C_3N_4/TiO_2 (Nanorods) composite

Color mapping shows homogenous distribution of all the elements over the catalyst surface. The ED spectra also confirm the presence of all the elements in the g-C_3N_4/TiO_2 (NR) composite.

4.1.5 X-Ray Diffraction Spectroscopy

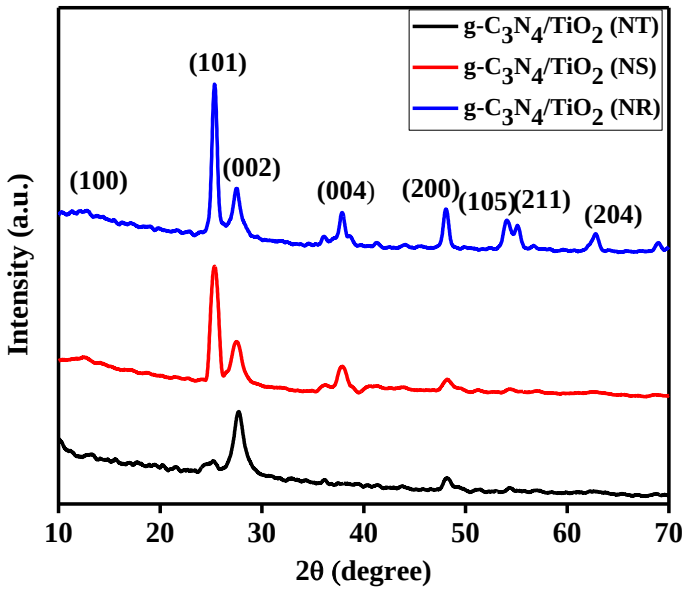

Fig. 4.1.5 XRD spectra of composite of g-C_3N_4 with TiO_2 (NT, NS, and NR)

Fig. 4.1.5 shows X-ray diffraction patterns of g-C_3N_4/TiO_2 (NT, NS, and NR) photocatalysts. The characteristic diffraction peaks of the TiO_2 observed at 2θ ~25.5°, 37.6°, 48.3°, 54.1°, 55.3° and 62.6° that correspond to (101), (004), (200), (105), (211) and (204) diffraction planes(JCPDS card No. 21-1272). Peaks corresponding to g-C_3N_4 can be observed around 2θ ~13.2°, and 27.9° and were related to the (002) and (100) planes (JCPDS 87-1526) of pure g-C_3N_4 (JCPDS card No. 21-1272) showing characteristic interlayer stacking structure. Presence of both types of peaks in composites spectra shows successful incorporation of g-C_3N_4 in TiO_2 but as the characteristic peaks of TiO_2 did not change this shows that g-C_3N_4 did not much disturbed the lattice of TiO_2[37].

4.2Photocatalytic Applications

4.2.1Photocatalysis

2 mg of g-C_3N_4/TiO_2 (P25, Nanospheres, Nanotubes, and Nanorods) was added in aqueous solution of Rhodamine B Dye (5ml of 5ppm). Firstly, stir the solution in complete dark for the first 20 minutes to attain an adsorption-desorption equilibrium. The reaction solution was then irradiated with visible light at different time intervals upto 80 minutes. Now, filter the catalyst using 0.45-µm nylon filters. UV-Vis spectrophotometer (Specord- 205 Analytik Jena) was used to observe the change in dye concentration (absorbance) [36]. The UV-Visible spectra of g-C_3N_4/TiO_2 (Nanorod) are shown in Fig.4.2.1a. To calculate the photodegradation efficiency following formula is used:

$R = \{(C_0 - C) / C_0\} \times 100 = \{(A_0 - A)/ A_0\} \times 100$

Table 4.2.1 Percent Degradation of C_3N_4 and different composites of g-C_3N_4 and TiO_2 in Rhodamine B Dye

	g-C_3N_4	g-C_3N_4/TiO_2 (P25)	g-C_3N_4/TiO_2 (Nanorods)	g-C_3N_4/TiO_2 (Nanotubes)	g-C_3N_4/TiO_2 (Nanospheres)
Percent Degradation	67.9%	74%	96.7%	94.5%	92%

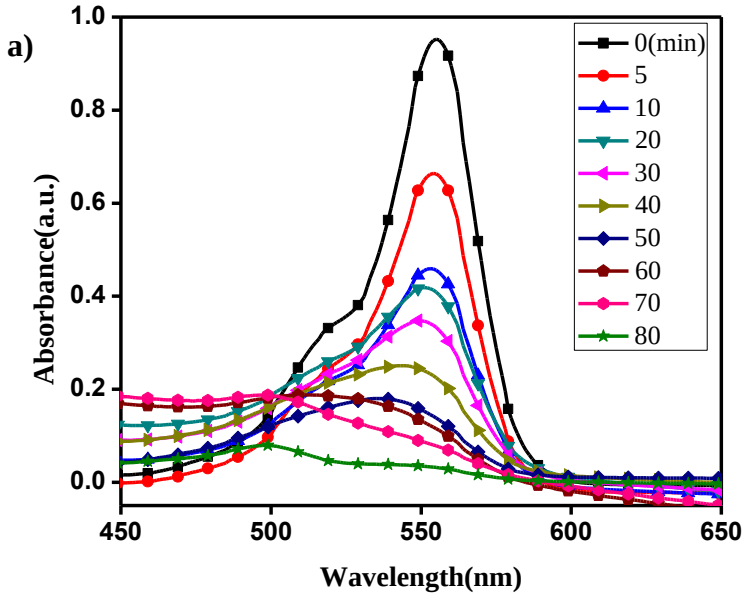

Fig. 4.2.1a UV-Visible Absorbance spectra of g-C_3N_4/TiO_2 (Nanorods) nanocomposite

The result from the above experiment shows that out of all the composites g-C_3N_4/TiO_2 (Nanorods) composite show the best catalytic activity. The percent degradation of the g-C_3N_4/TiO_2 (Nanorods) composite comes out to be 96.7% as calculated from the above formula. The percent degradation of other composites was also calculated by same method, their percent degradation values are shown in the Table 4.2.1.

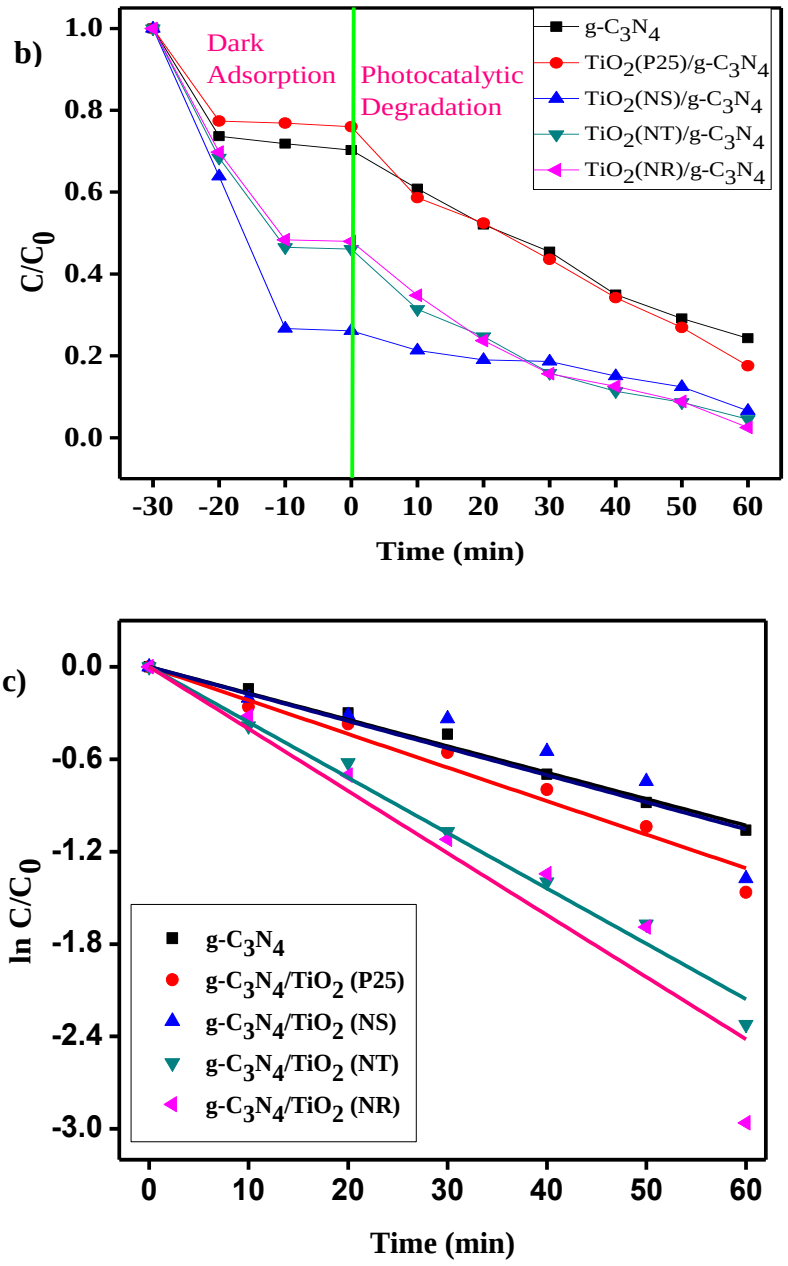

Fig. 4.2.2(b and c) Kinetic analysis of g-C_3N_4, and composite of g-C_3N_4 with P25, Nanorods (NR), Nanotubes (NT) and Nanospheres (NS)

4.2.2Reusability efficiency

Separation of the powder catalyst from the aqueous solution after dye degradation is one of the major problems. To avoid this, the best way is the reusability of the catalyst. Present catalysts are well dispersible under stirring and also easily separable from the solution. The catalyst can be easily separated from the dye solution as dye was not permanently adsorbed over the surface of catalyst. The separation of catalyst from dye solution can be easily done by centrifugation process.

By recycling the catalyst for several cycles, the effectiveness of the catalyst can be determined. Prior to use for another cycle, the catalyst was separated with the help of centrifugation process from the earlier cycle and then washed with water. It has been observed that there is a high photostability of g-C_3N_4/TiO_2 (NR) nanocomposite as seen from the experiments that the photocatalytic activity remains about constant even up to 5 successive cycles of the g-C_3N_4/TiO_2 (NR) photocatalyst as shown in Fig.4.2.2.

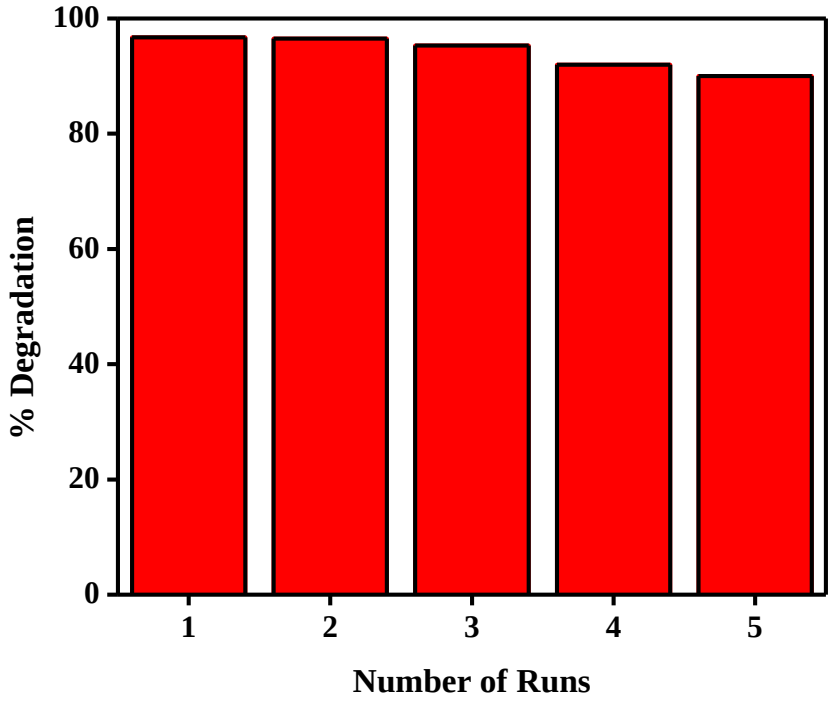

Fig.4.2.2 Reusability efficiency of g-C_3N_4/TiO_2 (Nanorods) nanocomposite for Rhodamine B Dye

4.2.3 Effect of pH on Photoactivity of catalyst

The activity of photocatalyst is greatly affected by the pH of dye solution. To observe the effect of pH of the solution on degradation efficiency of the present catalyst, solution of RhB dye has been prepared at different pH (of pH 1, 3, 5, 7, and 9). Desired amount of g-C_3N_4/TiO_2 (NR) catalyst (2 mg) was added to the solution of Rhodamine B dye (5 mL of 5ppm) at different pH and stir the reaction mixture to attain adsorption–desorption equilibrium for 20 min in complete dark. This reaction solution was then irradiated by visible light (64 W) for all the catalysts up to 80 min. Now, filter the catalyst using 0.45-μm nylon filters. UV-Vis spectrophotometer (Specord- 205 Analytik Jena) was used to observe the change in dye concentration (absorbance) [18]. The percent degradation graph at different pH is shown in Fig.4.2.3. To calculate the degradation efficiency following formula was used:

$R = \{(C_0 - C) / C_0\} \times 100 = \{(A_0 - A)/ A_0\} \times 100$

Where C_0 and C are the concentration

and A_0 and A are the absorbance of Rhodamine B dye at 0 and t reaction time, respectively.

The studies with present catalyst show that the catalyst is most effective in acidic pH especially at pH 3.

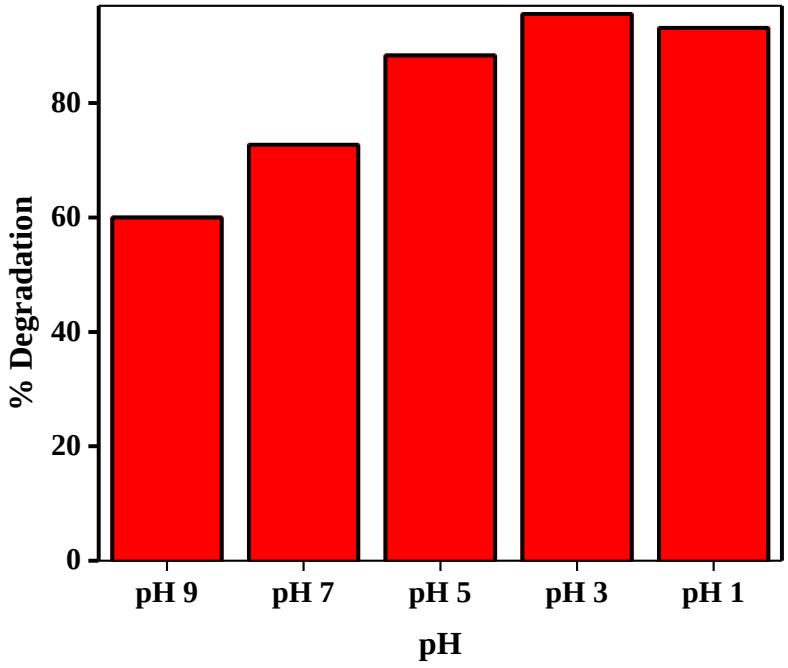

Fig.4.2.3 pH study of g-C_3N_4/TiO_2 (Nanorods) nanocomposite in Rhodamine B Dye

4.2.4 Effect of catalyst Concentration

Effect of Concentration of Catalyst determines the minimum and maximum amount of catalyst required for degradation. To study the effect of catalyst concentration on degradation of RhB dye different amount (2mg, 4mg, 6mg, 8mg, and 10mg) of g-C_3N_4/TiO_2 (NR) catalyst was added in aqueous solution of RhB dye (10ml of 5ppm) and then the solutions were stirred under the visible light (64 W) for 80 minutes. Now, filter the catalyst using 0.45-µm nylon filters. UV-Vis spectrophotometer was used to observe the change in dye concentration (absorbance).The observation shows that the efficiency of dye degradation increases as the concentration of catalyst increases from 2mg to 10mg in 10ml of dye solution. The increase in degradation efficiency is high when concentration of catalyst is increased upto 6mg after that the increase is comparatively less (from 6mg to 10mg). The C/C_0 graph at different catalyst concentration is shown below in Fig.4.2.4.

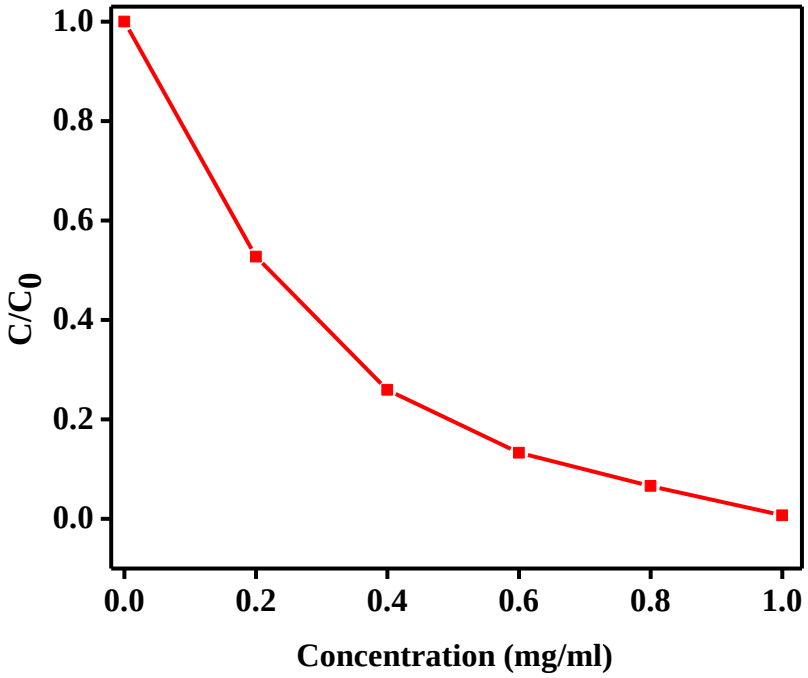

Fig.4.2.4 Concentration Study of g-C_3N_4/TiO_2 (Nanorods) nanocomposite in Rhodamine B Dye

4.2.5 Scavenger Study

Scavenger study with scavengers: Methanol, DMSO and Ascorbic Acid have been done with g-C_3N_4/TiO_2 catalyst. For this, 10^{-3} Molar solutions of all these scavengers have been prepared in Rhodamine B Dye solution. Desired amount of catalyst (2mg) was added in 5ml of the prepared solutions and the reaction was stirred under irradiation of visible light for 80 minutes. The degradation efficiency in each case was calculated and compared with the degradation efficiency in the absence of scavenger.

The present study with g-C_3N_4/TiO_2 (NR) photocatalyst shows that the degradation efficiency was most decreased in the presence of DMSO which tells that electrons play most important role in degradation (as DMSO scavenges electrons). Also degradation efficiency is highly decreased in presence of Ascorbic Acid scavenger (Ascorbic acid scavenges superoxide ion) showing the important role of superoxide ion in the degradation process. The degradation efficiency is least affected in case Methanol scavenger showing holes are less important for the reaction. The percent dye degradation in presence of different scavengers is shown in the graph below in Fig.4.2.5.

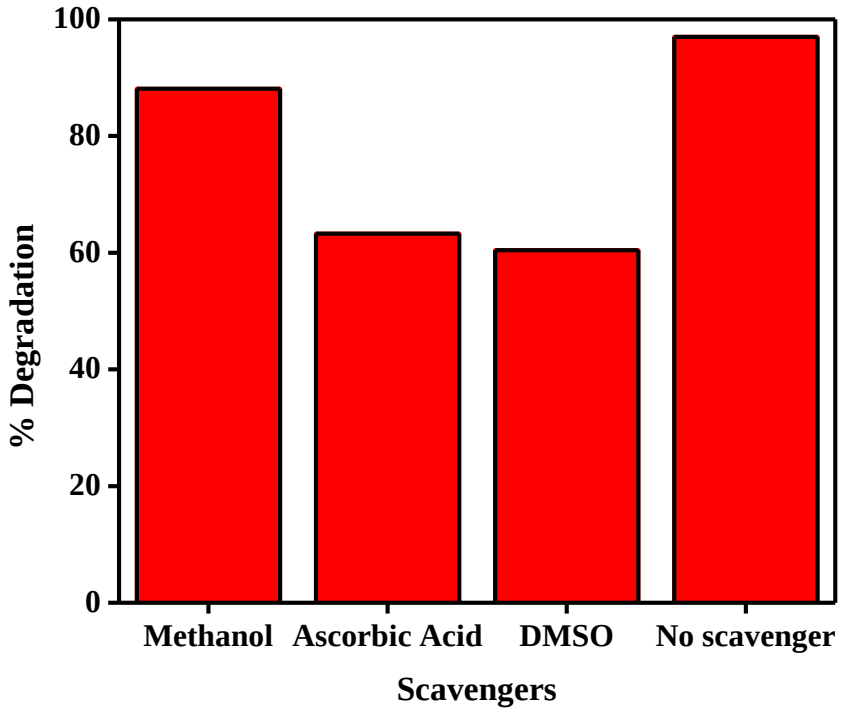

Fig.4.2.5 Scavenger study of g-C_3N_4/TiO_2 (NR) nanocomposite in Rhodamine B Dye

CHAPTER 5

Conclusion

Convenient and rapid synthesis of g-C_3N_4/TiO_2nanocomposites having different shapes of TiO_2 (Nanorods, Nanotubes, Nanospheres) had been carried out by different method and their photocatalytic activities were compared in respect to degradation of RhB dye. Characterization results show that TiO_2nanoparticles were embedded in the sheets of g-C_3N_4. From above study it is concluded that the photocatalytic efficiency of g-C_3N_4/TiO_2 nanocomposites is highly dependent on the shape of TiO_2. The nanocomposites of g-C_3N_4/TiO_2 (NS, NT, NR, and P25) show the higher photocatalytic activity than the pure g-C_3N_4 and TiO_2 under visible light. . The degradation efficiency ofg-C_3N_4/TiO_2 (NR) found to be (~97%) greater than composite of g-C_3N_4 with other shapes of TiO_2 (NS, NT and P25).The improvement in photocatalytic activity of composite is due to decrease in band gap energy and increased light absorption in visible region. Also there is an increase in electron hole separation efficiency due to effectual interfacial transfer of electron between g-C_3N_4 and TiO_2 (NR, NS, NT) of g-C_3N_4/TiO_2 composites. Due to their high reusability efficiency along with environment friendly nature, these nanocomposites may be used in sustainable development or other industrial applications.

CHAPTER 6

References

1. V. K. Gupta; Application of low-cost adsorbents for dye removal–A review. *Journal of environmental management*, **2009**, *90*(8), 2313-2342.
2. M. A. Rauf and S. S. Ashraf; Fundamental principles and application of heterogeneous photocatalytic degradation of dyes in solution. *Chemical engineering journal*, **2009,** *151*, 10-18.
3. J. Šíma and P. Hasal; Photocatalytic degradation of textile dyes in a TiO2/UV system. *Chemical Engineering*, **2013**, *32*, 79-84.
4. E. Forgacs, T. Cserhati, and G. Oros; Removal of synthetic dyes from wastewaters: a review. *Environment international*, **2004**, *30*(7), 953-971.
5. Y. Anjaneyulu, N. S. Chary and D. S. S. Raj; Decolourization of industrial effluents–available methods and emerging technologies–a review. *Reviews in Environmental Science and Bio/Technology*, **2005**, *4*(4), 245-273**.**
6. X. Zhang, Y. Wu, G. Xiao, Z. Tang, M. Wang, F. Liu and X. Zhu; Simultaneous photocatalytic and microbial degradation of dye-containing wastewater by novel g-C3N4-P25/photosynthetic bacteria composite. *PloS one*, **2017,** *12*(3), e0172747.
7. G. Booth, H. Zollinger, K. McLaren, W. G. Sharples and A. Westwell; Dyes, general survey. *Ullmann's Encyclopedia of Industrial Chemistry*, **2000**.
8. V. K. Gupta, D. Mohan, S. Sharma and M. Sharma; Removal of basic dyes (rhodamine B and methylene blue) from aqueous solutions using bagasse fly ash. *Separation Science and Technology*, **2000**, *35*(13), 2097-2113.
9. S. D. Richardson, C. S. Willson and K. A. Rusch; Use of rhodamine water tracer in the marshland upwelling system. *Groundwater*, **2004**, *42*(5), 678-688.
10. S. A. Khayyat, M. S. Akhtar, and A. Umar; ZnOnanocapsules for photocatalytic degradation of thionine. *Materials Letters*, **2012**, *81*, 239-241.

11. W. Z. Tang and H. An; UV/TiO2 photocatalytic oxidation of commercial dyes in aqueous solutions. *Chemosphere,* **1995**, *31*(9), 4157-4170.
12. M. H. Pérez, G. Peñuela, M. I. Maldonado, O. Malato, P. I. Fernández, I. Oller and S. Malato; Degradation of pesticides in water using solar advanced oxidation processes. *Applied Catalysis B: Environmental,* **2006**, *64*(3-4), 272-281.
13. M. Petala, V. Tsiridis, P. Samaras, A. Zouboulis and G. P. Sakellaropoulos; Wastewater reclamation by advanced treatment of secondary effluents. *Desalination,* **2006**, *195*(1-3), 109-118.
14. C. C. Liu, Y. H. Hsieh, P. F. Lai, C. H. Li and C. L. Kao; Photodegradation treatment of azo dye wastewater by UV/TiO2 process. *Dyes and Pigments,* **2006**, *68*(2-3), 191-195.
15. M. R. Hoffmann, S. T. Martin, W. Choi and D. W. Bahnemann; Environmental applications of semiconductor photocatalysis. *Chemical reviews,* **1995**, *95*(1), 69-96.
16. C. Y. Jimmy, J. Yu and J. Zhao; Enhanced photocatalytic activity of mesoporous and ordinary TiO2 thin films by sulfuric acid treatment. *Applied Catalysis B: Environmental,* **2002**, *36*(1), 31-43.
17. I. T. Peternel, N. Koprivanac, A. M. L. Božić and H. M. Kušić; Comparative study of UV/TiO2, UV/ZnO and photo-Fenton processes for the organic reactive dye degradation in aqueous solution. *Journal of hazardous materials,* **2007**, *148*(1-2), 477-484.
18. M. B. Mukhlish, F. Najnin, M. M. Rahman and M. J. Uddin; Photocatalytic Degradation of Different Dyes Using TiO 2 with High Surface Area: A Kinetic Study. *Journal of Scientific Research,* **2013**, *5*(2).
19. A. Mehta, M. Sharma, A. Kumar and S. Basu; Effect of Au content on the enhanced photocatalytic efficiency of mesoporous Au/TiO 2 nanocomposites in UV and sunlight. *Gold Bulletin,* **2017**, *50*(1), 33-41.
20. K. Sridharan, E. Jang and T. J. Park; Novel visible light active graphitic C3N4–TiO2 composite photocatalyst: Synergistic synthesis, growth and photocatalytic treatment of hazardous pollutants. *Applied Catalysis B: Environmental,* **2013**, *142*, 718-728.
21. S. Han, S. H. Choi, S. S. Kim, M. Cho, B. Jang, D. Y. Kim and T. Hyeon; Low-Temperature Synthesis of Highly Crystalline TiO2 Nanocrystals and their Application to Photocatalysis. *Small*, **2005**, *1*(8-9), 812-816.

22. H. Dong, G. Zeng, L. Tang, C. Fan, C. Zhang, X. He and Y. He; An overview on limitations of TiO2-based particles for photocatalytic degradation of organic pollutants and the corresponding countermeasures. *Water research*, **2015**, *79*, 128-146.
23. S. G. Kumar and L. G. Devi; Review on modified TiO2 photocatalysis under UV/visible light: selected results and related mechanisms on interfacial charge carrier transfer dynamics. *The Journal of physical chemistry A*, **2011**, *115*(46), 13211-13241.
24. W. Shi, F. Guo, J. Chen, G. Che and X. Lin; Hydrothermal synthesis of InVO4/Graphitic carbon nitride heterojunctions and excellent visible-light-driven photocatalytic performance for rhodamine B. *Journal of Alloys and Compounds*, **2014**, *612*, 143-148.
25. Y. Ji, J. Cao, L. Jiang, Y. Zhang and Z. Yi; G–C3N4/BiVO4 composites with enhanced and stable visible light photocatalytic activity. *Journal of Alloys and Compounds*, **2014**, *590*, 9-14.
26. J. Lei, Y. Chen, F. Shen, L. Wang, Y. Liu and J. Zhang; Surface modification of TiO2 with g-C3N4 for enhanced UV and visible photocatalytic activity. *Journal of Alloys and Compounds*, **2015**, *631*, 328-334.
27. S. Zuluaga, L. H. Liu, N. Shafiq, S. M. Rupich, J. F. Veyan, Y. J. Chabal, and T. Thonhauser; Structural band-gap tuning in gC 3 N 4. *Physical Chemistry Chemical Physics*, **2015**, *17*(2), 957-962.
28. J. Liu, T. Zhang, Z. Wang, G. Dawson and W. Chen; Simple pyrolysis of urea into graphitic carbon nitride with recyclable adsorption and photocatalytic activity. *Journal of Materials Chemistry*, **2011**, *21*(38), 14398-14401.
29. J. Qiu, Y. Feng, X. Zhang, X. Zhang, M. Jia, and J. Yao; Facile stir-dried preparation of gC 3 N 4/TiO 2 homogeneous composites with enhanced photocatalytic activity. *RSC Advances*, **2017**, *7*(18), 10668-10674.
30. H. Yan and H. Yang; TiO2–g-C3N4 composite materials for photocatalytic H2 evolution under visible light irradiation. *Journal of alloys and compounds*, **2011**, *509*(4), L26-L29.
31. X. Zhou, F. Peng, H. Wang, H. Yu and Y. Fang; Carbon nitride polymer sensitized TiO2 nanotube arrays with enhanced visible light photoelectrochemical and photocatalytic performance. *Chemical Communications*, **2011**, *47*(37), 10323-10325.
32. H. B. Fang, Y. Luo, Y. Z. Zheng, W. Ma and X. Tao; Facile Large-scale synthesis of urea-derived porous graphitic carbon nitride with extraordinary visible-light spectrum

photodegradation. *Industrial & Engineering Chemistry Research*, **2016**, *55*(16), 4506-4514.

33. S. Han, S. H. Choi, S. S. Kim, M. Cho, B. Jang, D. Y. Kim and T. Hyeon; Low-Temperature Synthesis of Highly Crystalline TiO2 Nanocrystals and their Application to Photocatalysis. *Small*, **2005**, *1*(8-9), 812-816.
34. S. Afshar and M. Hakamizadeh; Synthesis and characterisation of TiO2-derived nanotubes. *Journal of Experimental Nanoscience*, **2009**, *4*(1), 77-86.
35. R. A. Rather, S. Singh and B. Pal; A Cu+ 1/Cu0-TiO2 mesoporous nanocomposite exhibits improved H2 production from H2O under direct solar irradiation. *Journal of Catalysis*, **2017**, *346*, 1-9.
36. A. Mishra, A. Mehta, M. Sharma and S. Basu; Enhanced heterogeneous photodegradation of VOC and dye using microwave synthesized TiO2/Clay nanocomposites: A comparison study of different type of clays. *Journal of Alloys and Compounds*, **2017**, *694*, 574-580.
37. Z. Yang, J. Yan, J. Lian, H. Xu, X. She and H. Li; g-C3N4/TiO2 Nanocomposites for Degradation of Ciprofloxacin under Visible Light Irradiation. *Chemistry Select*, **2016**, *1*(18), 5679-5685.

Thesis

ORIGINALITY REPORT

6%	3%	5%	%
SIMILARITY INDEX	INTERNET SOURCES	PUBLICATIONS	STUDENT PAPERS

PRIMARY SOURCES

1	Akansha Mehta, Manu Sharma, Ashish Kumar, Soumen Basu. "Effect of Au content on the enhanced photocatalytic efficiency of mesoporous Au/TiO2 nanocomposites in UV and sunlight", Gold Bulletin, 2016 Publication	1%
2	Wee-Jun Ong, Lling-Lling Tan, Yun Hau Ng, Siek-Ting Yong, Siang-Piao Chai. " Graphitic Carbon Nitride (g-C N)-Based Photocatalysts for Artificial Photosynthesis and Environmental Remediation: Are We a Step Closer To Achieving Sustainability? ", Chemical Reviews, 2016 Publication	1%
3	dspace.thapar.edu:8080 Internet Source	1%
4	www.science.gov Internet Source	1%
5	library.cmu.ac.th Internet Source	1%

S. Basu

6	Sangjin Han. "Low-Temperature Synthesis of Highly Crystalline TiO2 Nanocrystals and their Application to Photocatalysis", Small, 08/2005 Publication	1%
7	pubs.acs.org Internet Source	1%

Exclude quotes	On	Exclude matches	< 1%
Exclude bibliography	On